Swelling-Induced Stresses in Ion-Bombarded Surfaces: Effect of Crystalline Orientation

W.G. Wolfer and F.A. Garner

February 1979

UWFDM-286

J. Nucl. Matls. 85 & 86, 583 (1979).

FUSION TECHNOLOGY INSTITUTE

UNIVERSITY OF WISCONSIN

MADISON WISCONSIN

Swelling-Induced Stresses in Ion-Bombarded Surfaces: Effect of Crystalline Orientation

W.G. Wolfer and F.A. Garner

Fusion Technology Institute
University of Wisconsin
1500 Engineering Drive
Madison, WI 53706

http://fti.neep.wisc.edu

February 1979

UWFDM-286

J. Nucl. Matls. 85 & 86, 583 (1979).

SWELLING-INDUCED STRESSES IN ION-BOMBARDED SURFACES: EFFECT ON CRYSTALLINE ORIENTATION

W.G. Wolfer

F.A. Garner*

January 1979

Nuclear Engineering Department
University of Wisconsin
Madison WI 53706 U.S.A.

*Westinghouse Hanford Company
Richland WA 99352 U.S.A.

UWFDM-286

Presented at the First Topical Meeting on Fusion Reactor Materials, Miami Beach FL, 29-31 January 1979

SWELLING-INDUCED STRESSES IN ION-BOMBARDED SURFACES: EFFECT OF CRYSTALLINE ORIENTATION

W. G. WOLFER[1] AND F. A. GARNER[2]

[1]Nuclear Engineering Department, University of Wisconsin, Madison, WI 53706 U.S.A.

[2]Westinghouse Hanford Company, Richland, WA 99352 U.S.A.

The state of stress in ion-bombarded specimens is analysed. The magnitude of the lateral compressive stresses is shown to depend on the ratio of the swelling rate to the creep rate compliance. The latter is given for three different mechanisms of irradiation creep in face-centered cubic crystals. Due to the dependence of the creep compliance on the crystal orientation, the lateral stresses in a given grain depend on its orientation with respect to the specimen surface. Detailed results are presented of the state of stress as a function of the grain orientation for all three irradiation creep mechanisms. These results are discussed in the context of blistering and step-height measurements.

1. INTRODUCTION

The implantation of ions into crystal surfaces produces volume changes in the penetrated layer. In the case of blistering, the volume expansion is caused by the change in the lattice parameter and by the formation of gas bubbles. For self-ion bombardment, the volume expansion is produced by void swelling. Regardless of its origin, the volume expansion must generate stresses within the bombarded layer. Their existence has recently been confirmed [1] by measuring the bending of a beam bombarded with He from one side. It has also been proposed [1,2,3] that these stresses are the driving force for blistering. In a recent experiment, Ivanov, et al., [4] have shown that a uniaxial tensile stress applied externally to the specimen does indeed affect the critical He-fluence at which blistering is observed. Tensile stresses at low levels increase the critical fluence, whereas higher tensile stresses induce flaking. At these higher stresses, the undamaged part of the specimen may have plastically strained, whereas the bombarded layer does not plastically deform easily because it is radiation-hardened. A differential expansion between the hardened and the virgin material, as produced by the external load, can then lead to flaking. Regardless of the interpretation of this experiment, however, it demonstrated that loading stresses on the first-wall of fusion devices will affect blistering.

The recent controversy on the mechanism of blistering has polarized the issue unduly. On the one hand, it is argued [1,2,3] that the lateral compressive stresses produce buckling of the bombarded layer. However, the mechanical models used for a quantitative assessment are surely too simple to apply to blistering. For example, it is not taken into account that the bombarded layer is at least partially attached to the underlying material rather than separated. Second, the lateral stress distribution may not be uniform throughout the layer, and it may not only depend on the amount of injected gas but on other parameters.

On the other hand, Evans [5] has argued that blister caps exhibit expansions between 5 and 15%, and that such a strain is too large to be contained as a lateral elastic compression prior to the buckling of the layer. We like to note that this large an expansion must certainly occur after the onset of buckling, and therefore, his main argument against the lateral stress model is not to the point. As an alternate model for blistering, Evans proposes a gas-driven process based on the fracture of the material between overpressurized bubbles. Although this mechanism is probably facilitating the detachment of the bombarded layer from the underlying material, it can not explain the observed relationship between blister diameter and blister thickness. Nor can this mechanism illuminate the effect of external stress on blistering. It is our opinion that for the latter two aspects the lateral stress build-up in the bombarded layer is crucial. For the actual detachment process, however, the mechanism proposed by Evans is an essential contributing factor.

In the present paper, we derive the lateral stresses produced in an ion-bombarded layer as a function of the grain orientation. When discussing the results in the context of blistering we shall assume that the critical fluence is larger the smaller the lateral stresses. We wish not to imply, however, that the lateral stress is the only driving force for blistering or that its magnitude alone determines the onset of blistering.

The swelling in the bombarded top layer is only one factor in the stress buildup. The other important factor is irradiation creep. For a material with isotropic creep behavior, it has recently been shown [6] that the lateral

stresses $\sigma_{11} = \sigma_{22} = \sigma$ (see Fig. 1 for the coordinate directions) are given by

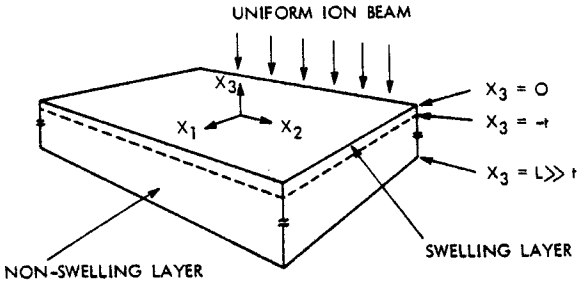

Fig. 1. Coordinate System Employed for Analysis of the Stress State in Ion-Bombarded Foils.

$$\sigma(x_3,t) = -\frac{\dot{S}}{\psi}\{1-\exp(-\frac{E\psi t}{3(1-\nu)})\} \qquad (1)$$

where $\dot{S}(x_3)$ is the local swelling rate, $\psi(x_3)$ $\sigma(x_3)$ is the local stress relaxation rate, E is the Young's modulus, and ν is the Poisson's ratio. The above equation is valid for material with isotropic elastic and creep properties, and for time-independent $\dot{S}$ and ψ. The additional assumption, namely that the stress relaxation rate is linear with stress, is strictly valid only for irradiation creep but not for thermal creep. Note that both $\dot{S}$ and ψ go to zero after stopping the irradiation. The residual value of σ is dependent on the last value of $\dot{S}/\psi$.

Equation (1) predicts that the lateral stress will reach a saturation value when the swelling rate $\dot{S}$ is balanced by the creep rate $\psi\sigma$.

How does this value depend on the irradiation conditions? If the lateral stress is important for blistering, why does is not lead to surface erosion under self-ion bombardment?

In order to shed some light on these questions we have investigated the effect of the crystal orientation (with regard to the specimen surface) on the lateral stress state. The motivation for this inquiry is twofold. First, it has been experimentally observed [7,8] that the appearance of blistering differs from grain to grain in a polycrystalline specimen. Analogous observation on differences in step-height from grain to grain have been made in self-ion bombardment experiments [9,10]. Garner, et al., [11] suggested that these differences in step-height are caused by the orientation dependence of the irradiation creep rate. A lower creep rate leads to a higher lateral stress and a correspondingly reduced swelling, provided swelling can be affected by stress. Second, all proposed mechanisms for irradiation creep do exhibit a dependence on the crystal orientation. Therefore, the dependence of blistering and of the step-heights on the grain orientation provides an important hint as to the dominant mechanism of irradiation creep under ion bombardment.

In the following sections we briefly summarize first the irradiation creep relationships for single crystals and for three deformation mechanisms. Then, we present the stress analysis in differently oriented crystal specimens. The obtained results are discussed in view of the above-mentioned experimental observation on blistering and step-heights.

2. THE IRRADIATION CREEP COMPLIANCE TENSOR

In crystalline solids, the relationship between the plastic strain rate tensor $\dot{e}_{ij}$ and the deviatoric stress tensor

$$s_{ij} = \sigma_{ij} - \frac{1}{3}\delta_{ij}\sigma_{kk} \qquad (2)$$

requires in general a fourth rank tensor $\psi_{ijk\ell}$, called henceforth the creep compliance tensor, to properly formulate a creep law. Hence,

$$\dot{e}_{ij} = \psi_{ijk\ell}\, s_{k\ell} \ . \qquad (3)$$

Here, and in the following, repeated indices indicate a summation; for example $\sigma_{kk} = \sigma_{11} + \sigma_{22} + \sigma_{33}$.

The creep compliance tensor has been evaluated for fcc metals and for three possible irradiation creep mechanisms: the stress-induced preferential absorption of point defects on faulted dislocation loops (SIPAL), the stress-induced preferential absorption on edge dislocations (SIPAD) or unfaulted loops, and the climb-controlled glide (CCG) of dislocations. For the SIPAL mechanism it was assumed that equal loop number densities exist on all four {111} planes. For the SIPAD and the CCG mechanisms the equivalent assumption was made that the dislocation densities for different Burger's and line vectors were identical. Furthermore, in the case of the CCG mechanism, the effect of stress on the climb rate was neglected in comparison with the radiation-induced climb rate.

In a coordinate system coincident with the cube edges of the fcc cell, called the crystal frame x_i^o, the irradiation creep compliance tensor can be written as [12]

$$\psi^o_{ijk\ell} = \psi\{\delta_{ik}\delta_{j\ell} + \delta_{i\ell}\delta_{jk} - \eta\,\delta_{ijk\ell}\} \qquad (4)$$

where δ_{ij} is the Kronecker symbol, $\delta_{ijk\ell}$ is equal to 1 if $i=j=k=\ell$, and zero otherwise. The scalar function ψ depends on the sink microstructure as well as the irradiation conditions. Hence, it also depends on which creep mechanism is dominant. The factor η assumes the following values

$$\eta = \begin{cases} 2 \text{ for SIPAL} \\ 1 \text{ for SIPAD} \\ -1 \text{ for CCG} \end{cases} \qquad (5)$$

To obtain the creep compliance tensor in any coordinate system, an orthogonal transformation

$$x_i = a_{ij}\, x_j^o$$

is carried out. Then, in the specimen frame

$$\psi_{ijk\ell} = a_{im}a_{jn}a_{kp}a_{\ell q}\psi^o_{mnpq} = \psi\{\delta_{ik}\delta_{j\ell}+\delta_{i\ell}\delta_{jk}-\eta \sum_{n=1}^{3} a_{in}a_{jn}a_{kn}a_{\ell n}\}. \quad (6)$$

3. STRESS ANALYSIS

Since the ion range is short compared to the specimen thickness, we may approximate a plane specimen bombarded uniformly with ions by a semi-infinite medium as indicated in Fig. 1. Swelling produces then a plane state of stress, i.e.,

$$\sigma_{33} = \sigma_{31} = \sigma_{32} = 0 \quad . \quad (7)$$

Furthermore, because of the constraint of the underlying material (which does not swell or expand) the lateral strains are zero everywhere with the exception near the specimen edges. Therefore,

$$\varepsilon_{11} = \varepsilon_{22} = \varepsilon_{12} = 0 \quad , \quad (8)$$

where ε_{ij} is the total strain tensor.

An unrestrained cubic crystal with no preferred orientation of the dislocation structure swells isotropically. Hence, the total strain rate is given by

$$\dot{\varepsilon}_{ij} = \dot{\varepsilon}^{e\ell}_{ij} + 1/3\ \delta_{ij}\ \dot{S} + \dot{e}_{ij} \quad (9)$$

where $\varepsilon^{e\ell}_{ij}$ is the elastic strain tensor. If we assume elastic isotropy, then

$$E\ \varepsilon^{e\ell}_{ij} = (1+\nu)\ \sigma_{ij} - \nu\delta_{ij}\ \sigma_{kk} \quad . \quad (10)$$

The Eq. (9) gives for the three conditions expressed by Eq. (8) the relations

$$\frac{1}{E}\dot{\sigma}_{11} - \frac{\nu}{E}\dot{\sigma}_{22} + \psi_{1111}\ s_{11} + 2\psi_{1112}\ s_{22} + \psi_{1122}\ s_{22} + \psi_{1133}\ s_{33} = -\frac{1}{3}\dot{S} \quad (11)$$

$$\frac{1}{E}\dot{\sigma}_{22} - \frac{\nu}{E}\dot{\sigma}_{11} + \psi_{2211}\ s_{11} + 2\psi_{2212}\ s_{12} + \psi_{2222}\ s_{22} + \psi_{2233}\ s_{33} = -\frac{1}{3}\dot{S} \quad (12)$$

$$\frac{1+\nu}{E}\dot{\sigma}_{12} + \psi_{1211}\ s_{11} + 2\psi_{1212}\ s_{12} + \psi_{1222}\ s_{22} + \psi_{1233}\ s_{33} = 0 \quad . \quad (13)$$

These equations can be integrated, and if the swelling rate and the creep compliance tensor are time-independent, the stresses build up according to time-functions of the form contained in Eq. (1). The stresses reach saturation levels which can be obtained from the Eqs. (11) to (13) for $\dot{\sigma}_{11} = \dot{\sigma}_{22} = \dot{\sigma}_{12} = 0$. To determine these saturation stresses we use Eqs. (2) and (7) in the above equations, and we obtain instead the following system of equations:

$$(2\psi_{1111} - \psi_{1122} - \psi_{1133})\ \sigma_{11} + 6\psi_{1112}\ \sigma_{12} + (2\psi_{1122} - \psi_{1111} - \psi_{1133})\ \sigma_{22} = -\dot{S} \quad (14)$$

$$(2\psi_{2211} - \psi_{2222} - \psi_{2233})\ \sigma_{11} + 6\psi_{2212}\ \sigma_{12} + (2\psi_{2222} - \psi_{2211} - \psi_{2233})\ \sigma_{22} = -\dot{S} \quad (15)$$

$$(2\psi_{1211} - \psi_{1222} - \psi_{1233})\ \sigma_{11} + 6\psi_{1212}\ \sigma_{12} + (2\psi_{1222} - \psi_{1211} - \psi_{1233})\ \sigma_{22} = 0 \quad (16)$$

We can eliminate σ_{12} by solving Eq. (16) and inserting the result in the other two equations. The latter contain only σ_{11} and σ_{22}, and their solution gives the final result:

$$\sigma_{11} = -\dot{S}\ (A_{22} - A_{12})/\Delta \quad (17)$$

$$\sigma_{22} = -\dot{S}\ (A_{11} - A_{21})/\Delta \quad . \quad (18)$$

Here

$$\Delta = A_{11}\ A_{22} - A_{12}\ A_{21} \quad , \quad (19)$$

and

$$A_{11} = 2\psi_{1111} - \psi_{1122} - \psi_{1133} - \psi_{1112}\ (2\psi_{1112} - \psi_{1222} - \psi_{1233})/\psi_{1212} \quad (20)$$

$$A_{22} = 2\psi_{2222} - \psi_{1122} - \psi_{2233} - \psi_{1222}\ (2\psi_{1222} - \psi_{1112} - \psi_{1233})/\psi_{1212} \quad (21)$$

$$A_{12} = 2\psi_{1122} - \psi_{1111} - \psi_{1133} - \psi_{1222}\ (2\psi_{1222} - \psi_{1112} - \psi_{1233})/\psi_{1212} \quad (22)$$

$$A_{21} = 2\psi_{1122} - \psi_{2222} - \psi_{2233} - \psi_{1222}\ (2\psi_{1112} - \psi_{1222} - \psi_{1233})/\psi_{1212} \quad . \quad (23)$$

For a given crystal orientation, the specimen surface normal vector can be characterized by a polar angle θ and azimuthal angle ρ relative to the crystal frame. The orthogonal transformation matrix is then given by

$$a_{ij} = \begin{pmatrix} \cos\rho & \sin\rho & 0 \\ -\sin\rho\ \cos\theta & \cos\rho\ \cos\theta & \sin\theta \\ \sin\rho\ \sin\theta & -\cos\rho\ \sin\theta & \cos\theta \end{pmatrix} \quad (24)$$

and the elements of the creep compliance tensor can be determined.

4. RESULTS

The saturation stresses for σ_{11}, σ_{22} and σ_{12} were computed for all orientations within the stereographic triangle, and are given in units of $\dot{S}/\psi$, where ψ is the scalar creep compliance in Eq. (6). Since $\dot{S}/\psi$ is unknown, only a relative comparison can be made among the stresses and orientation dependence for the same mechanism. Nevertheless, from previous work [13] we can conclude that the two mechanisms SIPAL and SIPAD give similar values for the scalar creep compliance ψ if the total loop line length equals the line dislocation density. Therefore, a rough comparison for these two mechanisms can also be made.

Figure 2 shows a contour plot of the shear

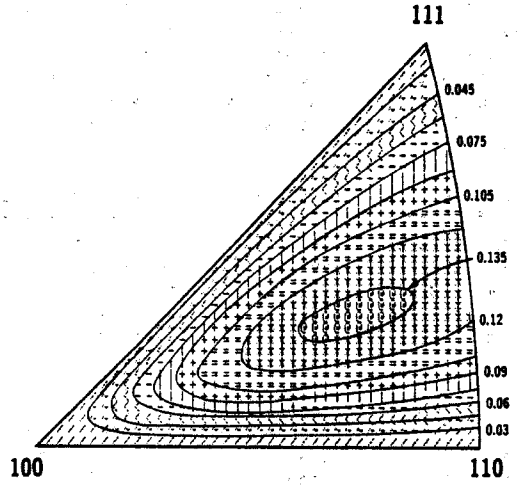

Fig. 2. The orientation dependence of the shear stress σ_{12} for SIPAD irradiation creep, given in units of $\dot{S}/\psi$.

stress σ_{12} for the SIPAD mechanism. Compared to the values of the two lateral normal stresses, σ_{11} and σ_{22}, the shear stress σ_{12} is always small. The same is true for the two other mechanisms though the distributions differ from the one in Fig. 2.

In the following Figures 3a, 4a, and 5a are shown the sum of the lateral stresses

$$\sigma_{\ell} = \sigma_{11} + \sigma_{22} \qquad (25)$$

and in Figures 3b, 4b, and 5b the maximum shear stress or equivalent stress

$$\tau_o = [\sigma_{11}^2+\sigma_{22}^2-\sigma_{11}\sigma_{22}+3\sigma_{12}^2]^{1/2} \qquad (26)$$

The Figures 3, 4, and 5 are for SIPAL, SIPAD, and CCG mechanism, respectively.

It can be seen from Fig. 3 that both σ_{ℓ} and τ_o become infinite in the case of SIPAL for any crystal orientations along the lower side of the stereographic triangle. These orientations correspond to situations where one of the [100] crystal axis is parallel to the specimen surface. If we choose this as the x_1-coordinate axis in the specimen frame, then the σ_{11} stress component cannot be relaxed by the SIPAL creep mechanism. The reason is that all {111} planes make the same angle with the x_1-direction, and hence, the loop bias factors are all equally affected by σ_{11}. The SIPA mechanism requires, however, that there be a difference in the bias factor for loops on different (111) planes.

For the "stiff" orientations, σ_{11} will build up until relaxation takes place by another deformation mechanism, i.e., ultimately by plastic flow or blistering.

No such "stiff" orientation is encountered with the two other mechanisms, SIPAD and CCG, and finite values are reached for both σ_{11} and σ_{22}. By comparing the values of both σ_{ℓ} and τ_o for the two SIPA mechanisms it is seen that SIPAL creep leads to larger compressive stresses than SIPAD creep even for orientation other than the "stiff" ones. Hence, a microstructure dominated by faulted dislocation loops gives rise to higher swelling-induced stresses.

Furthermore, creep according to SIPAD gives the least relaxation for [100]-oriented crystals, the most relaxation for [111] orientations, and intermediate relaxation for [110] orientations. In contrast, this order is reversed for creep by the CCG mechanism, and in addition, the relaxation is identical for [110] and [111] orientations.

5. DISCUSSIONS

The extent to which the three creep mechanisms are operative depends very much on the irradiation conditions, the temperature, and the microstructure resulting from the radiation damage and the gas concentration.

At low temperatures of irradiation, particularly under blistering conditions, the dislocation structure is dominated by small dislocation loops and small defect clusters. Both types of defects are very effective glide obstacles for the line dislocations. If these loops are of the faulted type, irradiation creep is likely to proceed according to the SIPAL mechanism with small contributions from the SIPAD and the CCG process. As we have seen, the stresses build up to rather high values in this case.

For fcc materials with high stacking fault energy, the loops are of the unfaulted type, and their contribution to the SIPA mechanism is included in the SIPAD process. Since the loops are capable of gliding in this case, they can more easily coalesce and reduce their density. Therefore, line dislocations may be able to glide more easily. It is then expected that creep proceeds by a combination of SIPAD and CCG.

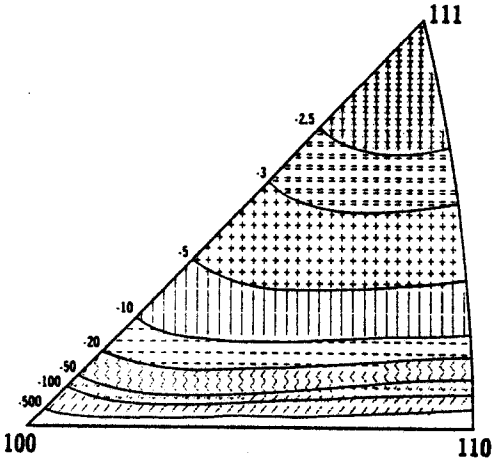

Fig. 3a. The orientation dependence of σ_ℓ for SIPAL irradiation creep, given in units of S/ψ.

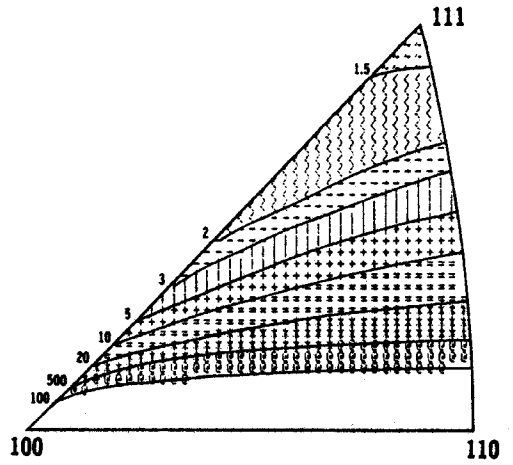

Fig. 3b. The orientation dependence of the maximum shear stress τ_o for SIPAL irradiation creep, given in units of S/ψ.

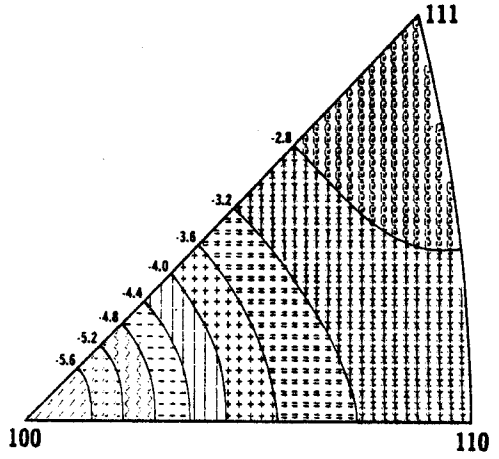

Fig. 4a. σ_ℓ for SIPAD irradiation creep.

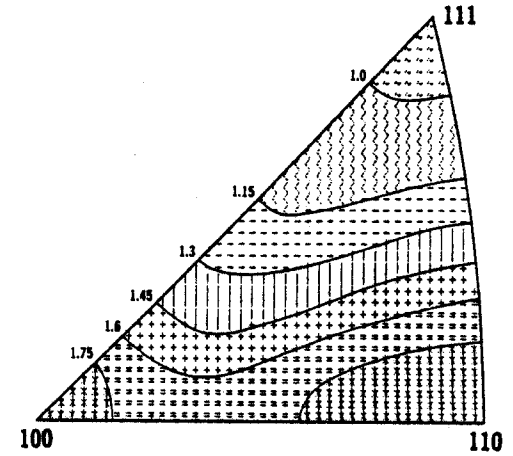

Fig. 4b. τ_o for SIPAD irradiation creep.

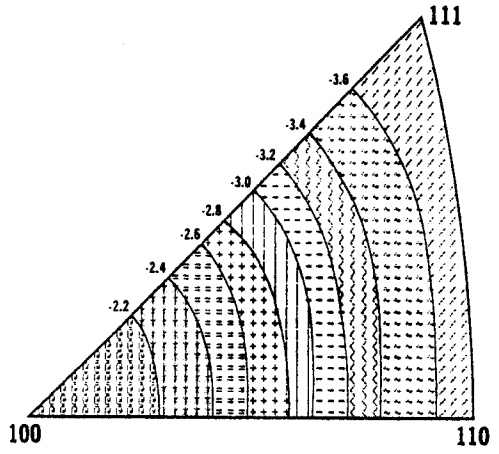

Fig. 5a. σ_ℓ for CCG irradiation creep.

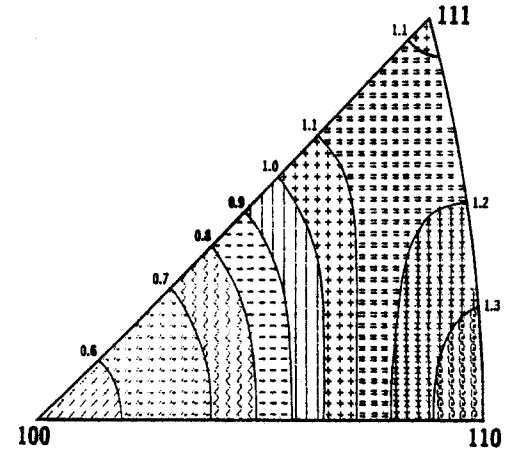

Fig. 5b. τ_o for CCG irradiation creep.

Whether these two creep processes take place independently of each other depends on the climb process. If climb can occur even in the absence of stress, SIPAD and CCG are not coupled. It is known that dislocation do climb while voids and bubbles grow.

Therefore, we expect that in the case of blistering, creep by SIPAD and CCG is simply additive, and the process which gives the most relaxation is the dominant one. As a result, CCG dominates for grains with [100] orientations, and SIPAD for grains w/ [111] orientations. This means that the additive combination of the two gives low lateral stresses for both [100] and [111] orientations, and hence reduced propensity for blistering. This conclusion agrees with the observations made by Milacek and Daniels [7] on blistering in Al, which, incidentally, is a high stacking fault material.

In contrast, when no void or bubble growth occurs, dislocation climb must be stress-induced. In this case, the CCG mechanism proceeds only when the SIPAL or the SIPAD mechanisms are also activated, and the creep process leading to the highest stress is rate-controlling. We believe that this situation may indeed be encountered during the incubation period for void nucleation in self-ion bombardment. Here, the low concentration of He is not sufficient for stable voids to form immediately. Instead, it takes time for a void population to build up, and the initial swelling rate is low in comparison to its value after incubation. Nevertheless, $\dot{S}$ is sufficiently large to cause the buildup in lateral stress (note that a linear expansion of 0.1% is all that is needed to produce a stress close to the yield stress when no relaxation occurs). Since $\dot{S}$ is small, the stress-independent climb rate of dislocations is small. Therefore, climb is really controlled by the SIPAD process, and the CCG process is coupled to SIPAD. In this case, we expect large lateral stresses for [100], [111], and [110] orientations, and lower values in between. Since compressive stresses retard void nucleation[14], the step-heights (being equal to swelling) should be lower for grains with these two orientations compared with orientation in between. Indeed, our conclusion is in qualitative agreement with step-height measurements on ion-bombarded stainless steel [9]. Furthermore, since the step-height difference develops largely during the incubation period, it should remain relatively constant afterwards. Again, the observations [10] seem to indicate that the step-height difference does not increase in proportion to the average step-height.

After the void incubation period, creep by SIPAD and CCG becomes uncoupled again and additive. Furthermore, as confirmed by irradiation creep experiments [15], ψ increases, and the lateral stress decreases.

It should be pointed out that self-ion bombardment experiments are in general performed at a much higher homologous temperature than the blistering experiments. Based on the neutron results [15], ψ can be estimated for self-ion bombardments, and lateral stress levels are predicted [6] to be at the most 0.2 to 0.3 MPa. At these high temperatures thermal creep can further reduce these stresses.

The condition in a fusion reactor device differs of course from the conditions studied in both blistering and self-ion bombardment. Whereas the ratio of He buildup to the displacement damage is very high for the former, it is very low for the latter. For a fusion reactor, it is in between.

There are some interesting corollaries of this work with regard to first walls in fusion reactors. First, the thermal stresses in a first wall, being compressive on the side facing the plasma, should contribute to the earlier onset of blistering. On the other hand, radiation damage caused by the neutrons should enhance the creep compliance ψ and thereby reduce the ratio of $\dot{S}/\psi$. The onset of blistering may then be delayed.

Second, external loads due to coolant pressure may sufficiently compensate the swelling-induced lateral stresses to reduce the tendency for blistering. If, however, the loads are too high, they may induce flaking, as suggested by the experiments of Ivanov et al. [4]. It is therefore important to obtain a further understanding of the effect of stress on blistering

This work was supported in part by the Division of Materials Science, U.S. Department of Energy, under contract ER-78-S-02-4861 with the University of Wisconsin, and by the Division of Reactor Development, under contract EY-76-C-14-2170 with Westinghouse Hanford Company.

REFERENCES

1. E.P. Eer Nisse and S.T. Picraux, J. Appl. Phys. 48 (1977), 9.

2. R. Behrisch, J. Bottiger, W. Eckstein, J. Roth, and B.M.U. Scherzer, J. Nuclear Matls. 56 (1975), 365.

3. M. Risch, J. Roth, and B.M.U. Scherzer, Proc. of Internat. Symp. on Plasma Wall Interaction, Jülich (1976), Pergamon Press, 1977, p. 391.

4. L.I. Ivanov, A.P. Komissarov, N.A. Machlin, V.N. Melnikov, and V.F. Chebaevsky, J. Nuclear Matls. 76 & 77 (1978), 211.

5. J.H. Evans, J. Nuclear Matls. 76 & 77 (1978), 228.

6. W.G. Wolfer, Proc. of Workshop on Correlation of Neutron and Charged Particle Damage, Oak Ridge Nat. Lab., 1976, CONF-760673, p. 369.

7. L.H. Milacek, and R.D. Daniels, J. Appl. Phys. 39 (1968), 5714.

8. H. Verbeek and W. Eskstein, in Applications of Ion Beams to Metals, ed. by S.T. Picraux, E.P. Eer Nisse, and F.L. Vook, Plenum Press, 1974, p. 597.

9. W.G. Johnson, J.H. Rosolowski, A.M. Turkalo, and K.D. Challenger, Scripta Metall. 6 (1972) 999.

10. A.L. Chang and R. Bajaj, private communication.

11. F.A. Garner, G.L. Wire, and E.R. Gilbert, in Proc. Internat. Conf. on Radiation Effects and Tritium Technology for Fusion Reactors, Gatlinburg (1975), CONF-750959, p. 474.

12. Details of the derivation will be published elsewhere.

13. W.G. Wolfer, Scripta Metall. 9 (1975), 801.

14. W.G. Wolfer, L.K. Mansur, and J.A. Sprague, Proc. Internat. Conf: Radiation Effects in Breeder Structural Materials, ed. by M.L. Bleiberg and J.W. Bennett, AIME (1977), p. 841.

15. E.R. Gilbert, J.L. Straalsund, and G.L. Wire, J. Nuclear Matls. 65 (1977), 266.